Theory and observations of low frequency eigenmodes due to Alfvén acoustic coupling in toroidal fusion plasmas*

N. N. Gorelenkov 1), E. Fredrickson 1), M.A. Van Zeeland 2), H. L. Berk 3), N. A. Crocker 4), D. Darrow 1), G.-Y. Fu 1), W.W. Heidbrink 5), S. Kubota 4), J. Menard 1), R. Nazikian 1), W.A. Peebles 4), M. Podesta 5), S. E. Sharapov 6) and JET-EFDA contributors [1]

1) Princeton Plasma Physics Laboratory, Princeton University
2) General Atomics, San Diego, California
3) IFS, Austin, Texas
4) University of California, Los Angeles
5) University of California, Irvine
6) Euratom/UKAEA Fusion Assoc., Culham Science Centre, Abingdon, Oxfordshire

*This work supported in part by the U.S. Department of Energy under the contracts DE-AC02-76CH03073 and DE-FG03-96ER-54346 and in part by the European Fusion Development Agreement

[1] *See the Appendix of F. Romanelli et.al., paper OV/1-2, this conference.*

Theory and observations of low frequency eigenmodes due to Alfvén acoustic coupling in toroidal fusion plasmas[2]

N. N. Gorelenkov 1), E. Fredrickson 1), M.A. Van Zeeland 2), H. L. Berk 3), N. A. Crocker 4), D. Darrow 1), G.-Y. Fu 1), W.W. Heidbrink 5), S. Kubota 4), J. Menard 1), R. Nazikian 1), W.A. Peebles 4), M. Podesta 5), S. E. Sharapov 6) and JET-EFDA contributors [3]

1) Princeton Plasma Physics Laboratory, Princeton University; 2) General Atomics, San Diego, California; 3) IFS, Austin, Texas; 4) University of California, Los Angeles; 5) University of California, Irvine; 6) Euratom/UKAEA Fusion Assoc., Culham Science Centre, Abingdon, Oxfordshire.

e-mail contact of main author: ngorelen@pppl.gov

Abstract. New theory developments and experimental observations of two classes of energetic particle driven instabilities are reported. First is a new class of global MHD solutions resulting from coupling of the Alfvénic and acoustic fundamental MHD oscillations due to geodesic curvature. These modes, predicted theoretically and numerically and called Beta-induced Alfvén-Acoustic Eigenmodes (BAAEs), have been recently observed in low beta JET, DIII-D and high beta NSTX plasmas [1, 2]. The second class is the instability of Reversed Shear Alfvénic Eigenmodes (RSAEs or Alfvén Cascades -ACs), which are shown to be suppressed due to strong plasma pressure in NSTX. A kinetic theory is required if the modes strongly interact with the Alfvénic continuum. Both RSAEs and BAAEs can potentially deteriorate the fast ion confinement in next step fusion plasmas, especially if excited together with multiple global TAE instabilities [3]. At the same time they can be used as a diagnostic tool for fast ion and safety factor profiles, a technique known as MHD spectroscopy.

Low frequency plasma oscillations due to the coupling of two fundamental MHD branches, Alfvénic and acoustic, have attracted a lot of interest in recent years. They can have deleterious effects on plasma performance due to fast ion loss and wall heat load, but can be used for the so-called MHD spectroscopy to diagnose plasma parameters such as safety factor profiles.

In a cylinder the ideal MHD Alfvénic and acoustic branches do not interact and their solutions are uncoupled (see Fig.1 [left]) because of their polarization, which is purely compressional plasma displacement of the acoustic branch and incompressible of the Alfvénic branch. In a torus Alfvénic and acoustic waves couple due to the toroidal effect and their polarization is mixed. Various gaps in the continuum emerge (see Fig.1 [right]), such as TAE gap due to m and $m+1$ Alfvénic (poloidal) harmonics

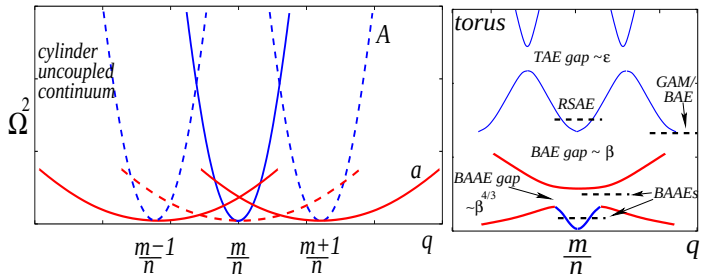

FIG. 1: *Schematic of the Alfvénic and acoustic continuum in a cylinder (left figure) and in a torus (right figure).*

[2] *This work supported in part by the U.S. Department of Energy under the contracts DE-AC02-76CH03073 and DE-FG03-96ER-54346 and in part by the European Fusion Development Agreement*

[3] *See the Appendix of F. Romanelli et.al., paper OV/1-2, this conference.*

coupling, beta-induced Alfvénic gap (BAE) due to the GAM induced up shift of the Alfvénic continuum, and beta-induced Alfvén - acoustic (BAAE) gap due to m Alfvénic and $m\pm1$ acoustic branches coupling, which was studied in detail recently [1, 2]. BAE and BAAE gaps are due to the geodesic curvature and finite plasma pressure. In each gap corresponding global eigenmode were found. In addition, global modes are found near the extrema points of the continuum, such as formed at the q_{min} location in the plasma with the reversed shear. Beta effects on two solutions shown in Fig.1, RSAE and BAAE are the subject of this work.

Plasma pressure effect on RSAEs is studied first by analyzing and modeling the experimental data from NSTX. RSAEs have been observed on many tokamak devices [4–7]. Most often RSAEs are observed with the frequency sweeping up as minimum $q(r)$ value, q_{min}, decreases. The RSAE frequency changes from a minimum stationary value to the TAE gap frequency [4]. Theoretically and numerically, it was found that sweeping up RSAEs exist in ideal MHD [8, 9]. RSAE instabilities with the frequency sweeping down are also observed prior to reaching the minimum. RSAE frequency is known to be determined by the four following terms

$$\omega_{RSAE}^2 = k_0^2 R_0^2 v_A^2 + \omega_{GAM}^2 + \Delta_{MHD}^2 + \Delta_h^2, \qquad (1)$$

where $k_j = (m+j-nq)/q$ is parallel wavevector [10], n is toroidal mode number, $\omega_{GAM} = \omega_A\sqrt{\gamma\beta_{pl}}$ is GAM (or BAE) frequency [11–13], Δ_{MHD} is a shift due to toroidicity and beta gradient (typically dominant) [14–16], and Δ_h is the hot ion contribution [10]. The plasma pressure influences the eigenfrequency via finite pressure, ω_{GAM}, and its gradient, Δ_{MHD}. Depending on plasma parameters the RSAE frequency pressure gradient contribution changes according to [17]

$$\frac{\Delta_{MHD}}{\omega_A} = -\frac{\pi^2}{2^3}\frac{r_0^2}{mqw^2} + \sqrt{\frac{\pi^4}{2^6}\frac{r_0^4}{m^2q^2w^4} + \frac{\alpha\varepsilon}{q^2}\left(1-\frac{1}{q^2}\right)} \le \sqrt{-r\beta'_{pl}(1-q^{-2})} = \frac{\omega_{GAM}}{\omega_A}\sqrt{-\frac{r\partial\beta}{\gamma\beta\partial r}(1-q^{-2})}, \qquad (2)$$

which is in agreement with numerical NOVA simulations for low beta, high aspect ratio plasma. In Eq.(2) the q-profile "width" is $w^2 = 2q/\left.q''\right|_{q=q_{min}}$.

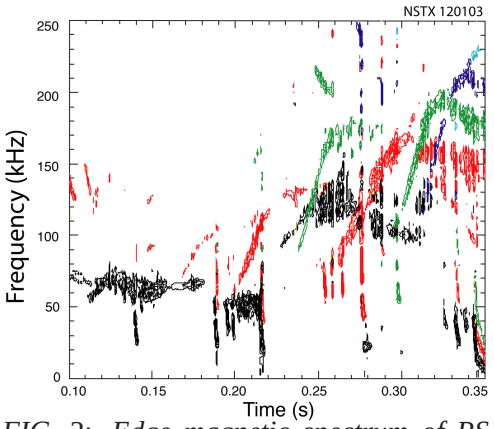

FIG. 2: Edge magnetic spectrum of RSAE instabilities in NSTX with $\beta_{pl} = 6\%$ at $t = 0.27s$, $R = 1.25m$. Color coding is black for $n = 1$, red for $n = 2$, and green for $n = 3$.

The study of RSAEs in NSTX was focused on the plasma pressure effects, which stabilize RSAE frequency sweep [6] via the GAM frequency up shift. The typical NSTX magnetic signal spectrum is shown in Fig. 2. The spectrum was taken at the initial phase of the shot when the plasma beta was building up, but was still relatively low for NSTX. Other plasma parameters are $n_{e0} = 10^{19}cm^{-3}$, $B = 4.5kG$ and plasma current of $0.8MA$. Conditions favorable for RSAE excitation were created with inverse $q-$profile and strong NBI heating with $2MW$ of $90keV$ beams. Instability of RSAEs has large upward frequency sweeps characteristic for observations in conventional tokamaks [5]. However, at higher plasma beta the RSAE frequency sweep is much reduced as can be seen from Fig. 3 (a). Corrected for the Doppler shift, instability frequency points (Fig. 3[b]) show familiar up and down sweeps, which are bounded by the TAE frequency from above and by $\sqrt{\omega_{GAM}^2+\Delta_{MHD}^2} \sim \beta_{pl}$ from below. For comparison, the GAM frequency is also shown as a black line in Fig.3(b). Near $t = 0.25sec$ we find that qualitatively Δ_{MHD}

is smallest for the lowest n value in agreement with predictions of Ref.[17], reaching maximum, Eq.(2), for higher n modes. At a later time, $t = 0.35sec$, q_{min} is close to unity as shown in Ref.[6], so that Δ_{MHD} vanishes (see Eq.[2]) and RSAE minimum frequencies approach f_{GAM} as in Fig.3(b). A further increase in plasma beta typically suppresses RSAE sweep.

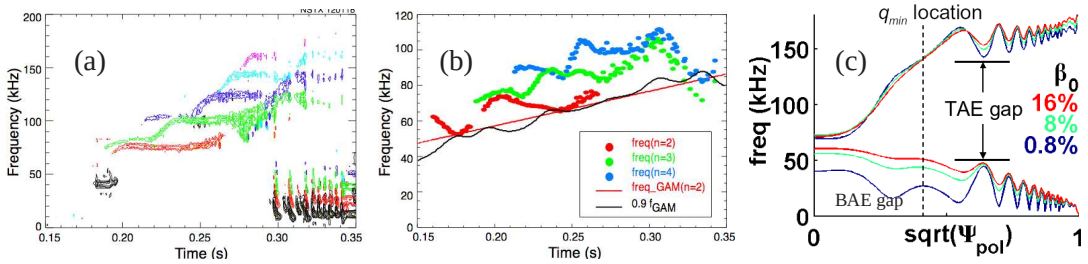

FIG. 3: *Figure (a) is the same as Fig. 2, except that* $\beta_{pl} = 11\%$. *Figure (b) shows the same frequency points, but accounted for the Doppler rotation at* q_{min} *surface. Figure (c) presents the NOVA continuum for a different central plasma pressure as a function of the plasma radius.*

RSAEs may induce significant beam ion losses in NSTX, especially when their instability is excited at the same time as TAE and form the "avalanches" [18].

Since theoretical expressions for RSAE eigenfrequency can give only approximate value in realistic plasma conditions we performed ideal MHD simulations using the NOVA code [19]. In these simulations acoustic mode coupling was included by neglecting acoustic continuum resonances in the ideal MHD model [12]. The main effect of acoustic mode coupling on shear Alfvén eigenmodes (SAEs) is retained resulting in a wider BAE gap (indicated in Fig.3[c]) and the up shift of each poloidal harmonic continuum frequency proportional to ω_{GAM}. Such a scheme simplifies the numerical procedure to search for the eigenmodes by filtering out dense acoustic interactions. Fig. 3 (c) shows the results of such modeling. The Alfvén continuum at the q_{min} location (RSAE localization region) up shift by the GAM frequency is proportional to the plasma beta as expected.

Thus the q_{min} change can only modify the narrow continuum between BAE and TAE gaps and should not result in an appreciable RSAE frequency sweep at high β_{pl}, i.e., the sweep is suppressed. Criteria for sweep suppression is when the GAM frequency becomes comparable to the TAE frequency [6]

$$\beta > (T_e + T_i)/4q^2 (7T_i/4 + T_e).$$

Further modeling of RSAE structure and frequency suggested that ω_{GAM} and Δ_{MHD} are on the same order in NSTX. This means that RSAEs excited at a $q_{min} = m/n$ interacts with TAE couplets $m = m'$ and $m' + 1$ at other radii $r_{m',n}$ where $q(r_{m',n}) = (m' + 1/2)/n$. The computed eigenmodes are formed by the coupling of TAEs and RSAE in NSTX because of strong coupling of corresponding poloidal harmonics of these modes. Notably the global structure of RSAE/TAE coupling in ST devices can be potentially dangerous for fast ion confinement. Thus the RSAE sweep suppression is a very important phenomena because it provides a mechanism to reduce fast ion - wave resonance island transport in phase space and potentially reduce radial transport of fast ions.

The BAAE theory was recently developed to predict and describe observations of new global eigenmodes in toroidal plasma experiments, such as presented here on JET, DIIID and NSTX devices. These modes appear near the continuum extrema points in the Alfvén-acoustic continuum gaps, which are formed by the interaction of Alfvén and acoustic branches mediated by finite pressure, plasma compressibility and geodesic curvature [20] (see illustration on Fig. 1 [b]). We

have found numerically that global BAAEs may occur adjacent to these extrema points in both relatively low and high beta plasmas. The question posed in initial studies [2] is whether kinetic theory can explain the frequency difference between ideal MHD and observations. The latter shows consistently lower values for the global BAAEs in the gap.

Qualitatively in ideal MHD and low beta, high aspect ratio plasmas the BAAE gap is limited from above by a frequency which appears when the $m\pm1$ acoustic sideband frequencies match $\Omega_{a+}=\Omega_{a-}$, and is given by [1, 20]

$$\Omega^2=\Omega_+^2=1/q^2, \tag{3}$$

where frequencies are normalized $\Omega^2\equiv\left(\omega R_0/v_A\right)^2/\delta$, $\delta\equiv\gamma\beta/2\ll1$, $\Omega_{a\pm}=k_{\pm1}$, and γ is the specific heat ratio. Near the rational magnetic surface another root, the modified Alfvén branch, "shielded" by the acoustic sidebands was found

$$\Omega^2=k_0^2/\delta\left(1+2q^2\right). \tag{4}$$

Theory predicted that if q_{min} decreases at that location the modified Alfvén branch frequency sweeps up until it reaches the acoustic frequency, which approximately constitutes the lower BAAE gap $\Omega_-^2=k_{-1}^2=k_0^2/\delta\left(1+2q^2\right)$ (see Fig.1(b)). Corresponding global solutions were found numerically. At $k_0^2>\delta$ the acoustic ±1 sideband solutions exist.

Straightforward application of the ballooning formalism to the frequencies of interest based on the quasi-neutrality condition and Amper's law result in the general dispersion relation applicable for the Alfvén-acoustic continuum

$$2-\sum_{\pm1}k_{\pm1}^{-2}\left\{\frac{\left[\xi_{\pm1i}+\left(\frac{1}{2}+\xi_{\pm1i}^2\right)Z_{\pm1}\right]^2}{\tau^{-1}+1+\xi_{\pm1i}Z_{\pm1}}-\left[\frac{3}{2}+\xi_{\pm1i}^2+\left(\frac{1}{2}+\xi_{\pm1i}^2+\xi_{\pm1i}^4\right)\frac{Z_{\pm1}}{\xi_{\pm1i}}\right]\right\}=\frac{2k_0^2}{\Omega^2\delta_k}, \tag{5}$$

which, if contributions from two acoustic sidebands are considered to be the same, $k_{+1}^2\simeq k_{-1}^2$ or $k_0\ll1/q$, is reduced to the dispersion obtained in Ref.[21], where the derivation of Eq.(5) is described. Here $\tau=z_i^2T_en_i/z_e^2T_in_e$, $\delta_k=\beta_i\tau/2$, $\xi_{\pm1i}=\omega/k_{\pm1}v_{Ti}$, $Z=Z\left(\xi_{\pm1i}\right)\equiv\pi^{-1/2}\int e^{-t}dt/\left(t-\xi_{\pm1i}\right)$, v_{Ti} is thermal ion velocity. We note that ±1 sideband contributions should be separated to recover MHD results.

Kinetic dispersion of the modified Alfvén branch in a plasma with dominant electron beta recovers ideal MHD BAAE gap, Eq.(4), if $\tau>2\xi_i^2\gg1$. In this case from Eq.(5) we find

$$\frac{k_0^2}{\Omega^2\delta_k}\simeq1+\frac{2q^2}{1-\xi_s^2}\left(1+\xi_s^3\tau^{3/2}e^{-\xi_s^2\tau/2}\frac{i\sqrt{\pi}\sigma}{4\sqrt{2}}\right), \tag{6}$$

where we used $\xi_i=\omega qR/v_{Ti}=\omega q\sqrt{\tau}/\omega_A\sqrt{\beta_e}\equiv\xi_s\sqrt{\tau/2}$. If its imaginary part is neglected it is reduced to the MHD dispersion and corresponds to the sweeping up BAAE solution when q decreases. The damping of this branch is exponentially small.

Another analytically treatable case is when T_i, or τ, is finite, and $\xi_{\pm i}\ll1$. We find then

$$\frac{k_0^2\omega}{\Omega^2\delta_k\left(\omega-\omega_{*pi}\right)}\simeq1+q^2\left(\frac{1}{2}+\frac{\pi}{4}\frac{\tau}{1+\tau}\frac{\left(\omega-\omega_{*i}-\omega_{*Ti}/2\right)^2}{\omega\left(\omega-\omega_{*pi}\right)}\right)+\frac{\omega-\omega_{*i}-3\omega_{*Ti}/2}{\omega-\omega_{*pi}}\frac{iq^2\sqrt{\pi}e^{-\xi_s^2\tau/2}}{\xi_s\sqrt{2\tau}}, \tag{7}$$

where we also included drift frequencies based on results of Ref.[21], $\omega_{*j} = nqv_{Ti}^2/2\omega_{ci}rL_j$, L_j is the gradient scale length computed for pressure, density, and temperature profiles for $j = pi, i, Ti$ respectively. This solution is strongly ion Landau damped due to the acoustic branch, assuming thermal ion parallel velocity is not changed over the characteristic time of the interaction with the mode. This is true if the bounce frequency of thermal ions is smaller than the mode frequency, that is $\sqrt{\beta_i\varepsilon} < Rk_{||}$, which can be satisfied for sufficiently small ε and plasma pressure. However, when temperature gradient is sufficiently large one can expect that BAAE instability is purely driven by thermal ions.

Eq.(5) also contains acoustic branches which correspond to a zero denominator of the second term in the curl brackets on the LHS. This branch is the same as in MHD, Eq.(3), for $\tau \gg 1$, but needs to be obtained numerically otherwise. Figure 4 shows the comparison of these limiting cases with MHD and with the general dispersion. The numerical evaluation of Eq.(5) shows that the damping rate of its branches increases rapidly when $\tau < 2$. Quantitatively in such a case the damping rate of the extremum points of the BAAE continuum is $\gamma/\omega >\sim 25\%$. The modified Alfvén branch damping becomes comparable to the frequency at smaller frequencies.

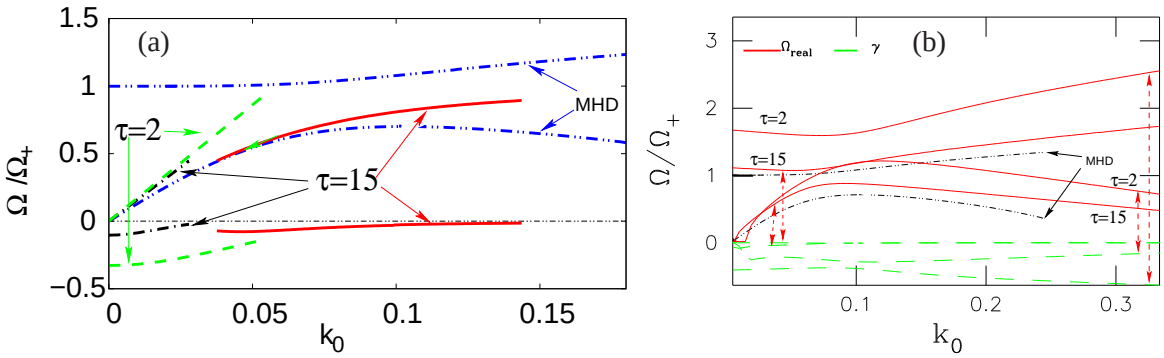

FIG. 4: BAAE continuum solutions comparison with the MHD solution as indicated. All real frequencies are positive and their imaginary parts are negative. Frequencies are normalized to $\Omega_+ = \omega_A\sqrt{\tau\beta_i/2}/q$ *for kinetic solution. MHD frequencies are normalized to* $\Omega_+ = \omega_A\sqrt{\gamma\beta/2}/q$*. On figure (a) two kinetic branches are shown for* $\tau = 15$*, lower frequency, Eq.(7), and higher frequency, Eq.(6) solutions. Eq.(7) dispersion is also shown for* $\tau = 2$*. Figure (b) presents frequencies evaluated using general dispersion relation, Eq.(5). Results are shown for* $n = 12$*,* $m = 21$ *and* $\delta = \delta_k = 0.25\%$*.*

In JET experiments instabilities with basic BAAEs properties were observed [1] (shown in Fig. 5 [a]), where low frequency magnetic activity was observed with the characteristic frequency sweep up. However, the frequency of $n = 4$ gap BAAE was found to be ~ 1.8 times higher than measured. In the original work it was assumed that the q-profile is monotonic and $\tau = 1$. A rather simple way to resolve this frequency mismatch was suggested in Ref.[2]. It was proposed that local low (and perhaps reversed) shear region with $q_{min} = 1.5$ exists. In that case we evaluate $\Omega_+ \simeq 21kHz$, so that the inferred gap BAAE frequency $\sim 16kHz$ becomes sufficiently close to the Doppler shifted observed $f = 14kHz$. This conjecture is supported by the presence of only even toroidal mode numbers, which follows from the requirements that $m = q_{min}n$ must be integer. Kinetic expressions in JET plasma conditions agree with ideal MHD because $\delta_k = \beta_e/2 = \delta$, since $\beta \simeq \beta_e$ and $\gamma \simeq 1$ for strongly ICRF heated plasma, when most of the energy of H-minority is transferred to electrons. It is also consistent with our kinetic model because as can be seen from Fig.5(a) modes are observed with very low frequency when theory predicts strong damping unless $\tau \gg 1$.

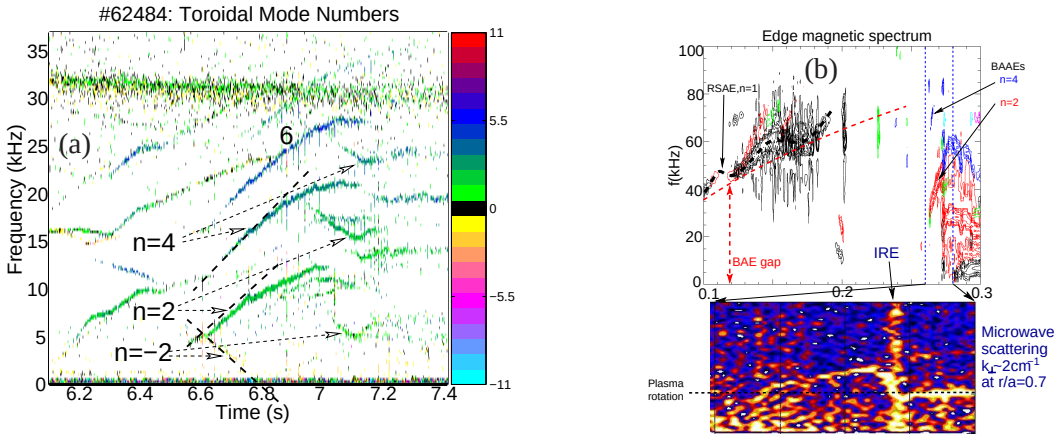

FIG. 5: *The magnetic signal frequency spectrum in JET (a) and NSTX (b). Different colors represent toroidal mode numbers according to the color chart on the right (figure [a]). Black dashed lines are tangential to the signal initial evolution at* $t = 6.6sec$. *In NSTX after RSAEs with slow evolving activity suppressed at* $t = 0.18s$, *the BAAE becomes unstable at* $t = 0.26s$, *such as* $n = 2$ *(red) and* $n = 4$ *(blue). BAAEs are also observed on the high-k scattering diagnostic shown in the insert (lower right).*

Magnetic spectrum in NSTX is shown in figure 5(b) at $n = 2,4$. The BAAE frequency sweeps up from the level of plasma rotation ($f_{rot} \simeq 15kHz$) at q_{min} surface to about $50kHz$ (for $n = 2$ mode) in the lab frame. In that shot the following parameters were achieved (at $t = 0.26s$) $R_0 = 0.855m$, $a = 0.66m$, $\beta_{pl0} \equiv 2\pi p(0)/B_0^2 = 0.34$, vacuum magnetic field at the geometrical center $B_0 = 0.44T$, edge and central safety factor values are $q_1 \simeq 13.86$ and $q_0 \simeq 2.1$. After an internal reconnection event (IRE) at $t = 0.275s$ the BAAE frequency goes down to the level of plasma rotation frequency. This may indicate that the q_{min} value is changed back to its value at $t = 0.262s$. Another interesting observation is that like in JET plasma only even n-number BAAEs have been observed at $t = 0.262 - 0.275s$. Independent MSE measurements indicate that q_{min} indeed is close to $3/2$. Detailed measurements of BAAE internal structure revealed the same radial localization, eigenfrequency (within measured accuracy) and their evolution as was predicted by ideal MHD theory. On the other hand, unlike JET observations, BAAEs in NSTX typically seem to stay near the modified Alfvén continuum frequency and do not enter the Alfvén-acoustic gap, which is predicted to be at $\sim 25kHz$ and is consistently above measured frequencies. In NSTX plasma $\tau \sim 1$ so that BAAE instability is possible only if the drive is strong. This is possible because fast ion pressure is comparable with the pressure of thermal ions. We note that the observed BAAEs in NSTX can form avalanches during which several modes are excited simultaneously and result in strong beam ion redistribution and loss of a neutron signal by 13%, which approximately indicate beam ion loss [22].

In dedicated experiments on DIII-D BAAE oscillations were also observed. Detailed measurements of internal low frequency oscillations shown in Figure 6(a) with the BES diagnostics reveal very low frequency peaks below the characteristic RSAE frequency signal, which we identified as BAAEs.

Experiments were conducted with the ECH applied at $0.8sec$ after which a strong broadband oscillations are seen in Figure 6(a). At a later time T_e increases, $\tau \sim 2$, and narrow BAAE peaks are seen in both BES and ECE spectra. These modes have localized radial structure near q_{min}. At $t = 1.6sec$ plasma is characterized by $R_0 = 1.66m$, $a = 0.64m$, $\beta_{pl0} = 5\%$, $B_0 = 2T$, $q_1 \simeq 6$,

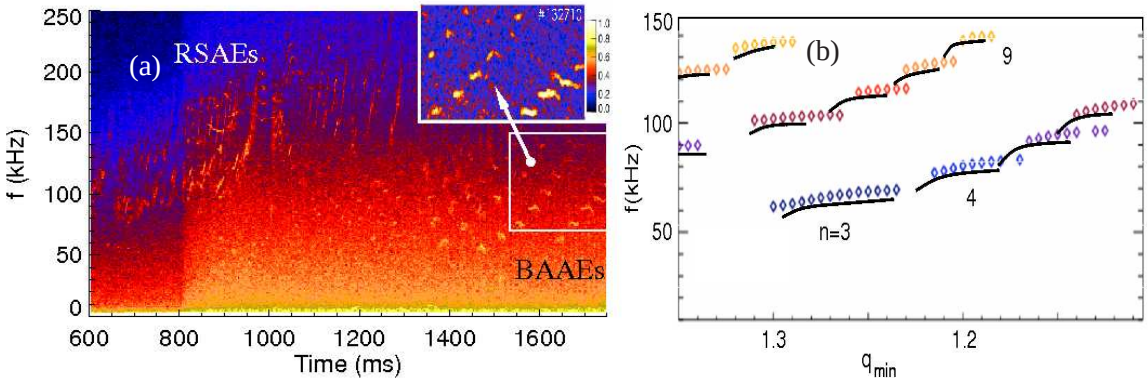

FIG. 6: *BES measured frequency spectrum (a) DIII-D shot* #132710 *and a zoom of a narrow region of several BES channels cross correlation shown in the insert. Figure (b) shows the results of NOVA simulations (points) of different n modes as indicated. Under each mode pointe shown as the black line is the lower continuum gap frequency from kinetic dispersion.*

$q_{min} \simeq 1.25$.

In order to identify the observed instabilities we have performed a search for eigenmodes using the NOVA code and have found gap solutions with the frequencies shown in Figure 6(b), which include the Doppler correction due to the plasma rotation $11.5kHz$ at q_{min}. NOVA finds solutions only as gap modes. During the sweeping up phase (modified Alfvén branch) all numerical solutions strongly interacted with the continuum and were discarded. Kinetic branch dispersion relation frequencies are also plotted, but for those values for which thermal ion Landau damping, Eq.7, satisfies $\gamma/\omega < 0.25$ and $0 < k_0 < 0.25$. Kinetic frequencies are plotted as sweeping up solutions transitioning to the gap frequency.

NOVA solutions turn out to be surprisingly close to the kinetic continuum gap frequency. They also show similar time duration to those observed (see insert on Fig. 6 [a]). The sequence of instabilities is also reproduced. However, in the experiments there were no discernible BAAE activity on edge magnetics so a toroidal mode number determination was not possible. Thus one can only check how consistent the predictions are with the data. In the modeling the BAAE gap frequency is on the order $30-40kHz$. Additional analysis of BES poloidal wavevector measurements and the mode frequencies shows that the instability frequency will be the subject of future work but preliminary analysis shows that the instability frequency is in the range $0-30kHz$.

Additionally, FIDA measurements of the beam ion profiles suggest that BAAEs increase fast ion transport on a level comparable to that due to RSAEs in DIII-D discharges [23].

In summary we demonstrated the effects of the acoustic branch on the low frequency Alfvénic oscillations in toroidal plasmas with the reversed safety factor. We have shown that due to large plasma beta in NSTX, characteristic frequency sweeping of RSAEs is suppressed. RSAEs are often stabilized by the finite pressure. New low frequency modes are studied and observed in JET, NSTX and DIII-D. They exist in the BAAE gap with the frequency below GAM. BAAEs induce losses of beam ions and forms avalanches in NSTX. Kinetic theory of BAAEs is formulated. It is shown that gap BAAEs are usually have smallest Landau damping in comparison with the sweeping up modes. If electron temperature exceeds thermal ion temperature BAAE dispersion is

close to the MHD and has weak damping. Observed BAAE frequencies within the experimental uncertainty agree with theory. With proper frequency normalization ideal MHD produces similar BAAE gap and can be used to simulate BAAE mode structure.

[1] N. N. Gorelenkov, H. L. Berk, E. Fredrickson, and S. E. Sharapov, Phys. Letters A **370/1**, 70 (2007).

[2] N. N. Gorelenkov, H. L. Berk, N. A. Crocker, E. D. Fredrickson, S. Kaye, S. Kubota, H. Park, W. Peebles, S. A. Sabbagh, S. E. Sharapov, et al., Plasma Phys. Control. Fusion **49**, B371 (2007).

[3] E. D. Fredrickson, R. E. Bell, D. Darrow, G. Fu, N. N. Gorelenkov, B. P. LeBlanc, S. S. Medley, J. E. Menard, H. Park, A. L. Roquemore, et al., Phys. Plasmas **13**, 056109 (2006).

[4] S. E. Sharapov, B. Alper, H. L. Berk, D. N. Borba, and et. al, Phys. Plasmas **9**, 2027 (2002).

[5] R. Nazikian, B. Alper, H. L. Berk, D. Borba, and et.al., in *Proceedings of 20th IAEA Fusion Energy Conference, Vilamoura, Portugal* (2004), IAEA-CN-116/EX/5-1, pp. 1–9.

[6] E. D. Fredrickson, N. A. Crocker, N. N. Gorelenkov, W. W. Heidbrink, S. Kubota, F. M. Levinton, H. Yuh, J. E. Menard, and R. E. Bell, Phys. Plasmas **14**, submitted (2007).

[7] M. A. V. Zeeland, W. W. Heidbrink, R. Nazikian, W. M. Solomon, M. E. Austin, H. L. Berk, N. N. Gorelenkov, C. T. Holcomb, A. W. Hyatt, G. J. Kramer, et al., Plasmas Phys. Control. Fusion **50**, 035009 (2008).

[8] B. N. Breizman, H. L. Berk, M. S. Pekker, S. D. Pinches, and S. E. Sharapov, Phys. Plasmas **10**, 3649 (2003).

[9] G. J. Kramer, R. Nazikian, B. Alper, M. de Baar, and et. al., Phys. Plasmas **13**, 056104 (2006).

[10] H. L. Berk, D. N. Borba, B. N. Breizman, S. D. Pinches, and S. E. Sharapov, Phys. Rev. Letters **87**, 185002 (2001).

[11] C. Z. Cheng, Phys. Fluids B **2**, 1427 (1990).

[12] M. S. Chu, J. M. Greene, L. L. Lao, A. D. Turnbull, and M. S. Chance, Phys. Fluids B **11**, 3713 (1992).

[13] B. N. Breizman, S. E. Sharapov, and M. S. Pekker, Phys. Plasmas **12**, 112506 (2005).

[14] G. J. Kramer, N. N. Gorelenkov, R. Nazikian, and C. Z. Cheng, Plasma Phys. Contr. Fusion **46**, L23 (2004).

[15] G. Y. Fu and H. L. Berk, Phys. Plasmas **13**, 052502 (2006).

[16] N. Gorelenkov, G. Kramer, and R. Nazikian, Plasma Phys. Control. Fusion **48**, 1255 (2006).

[17] N. N. Gorelenkov, E. D. Fredrickson, G. J. Kramer, R. Nazikian, and L. E. Zakharov, in *21st US Tokamak Transport Force Workshop, Boulder, Colorado: http://fusion.gat.com/conferences/ttf08* (Office of Science, DOE, 2008), to be published. PPPL Preprint 4340.

[18] E. D. Fredrickson and et.al, in *Proceedings of 22nd IAEA Fusion Energy Conference, Geneva, Switzerland* (2008), IAEA-CN-116/EX/41, pp. 1–9.

[19] C. Z. Cheng, Phys. Reports **211**, 1 (1992).

[20] B. van der Holst, A. J. C. Beliën, and J. P. Goedbloed, Phys. Plasmas **7**, 4208 (2000).

[21] F. Zonca, L. Chen, and R. Santoro, Plasma Phys. Contr. Fusion. **38**, 2011 (1996).

[22] D. Darrow, E. Fredrickson, N. Gorelenkov, A. Roquemore, and K. Shinohara, Nucl. Fusion **48**, 1 (2008).

[23] W. W. Heidbrink, N. N. Gorelenkov, Y. Luo, M. A. V. Zeeland, R. B. White, M. E. Austin, K. H. Burrell, G. J. Kramer, M. A. Makowski, G. R. McKee, et al., Phys. Rev. Lett. **99**, 245002 (2007).